

LOW COST ATTITUDE AND HEADING SENSORS IN TERRESTRIAL PHOTOGRAMMETRY – CALIBRATION AND TESTING

Jakub Kolecki¹, Przemysław Kuras²

^{1,2} Faculty of Mining Surveying and Environmental Engineering, AGH University of
Science and Technology, Poland - (kolecki, kuras)@agh.edu.pl

KEY WORDS: Direct geo-referencing, IMU, GPS/INS, Bundle adjustment, Sensor calibration, Accuracy test

ABSTRACT: Most of the contemporary terrestrial mobile mapping systems (MMSs) use tactical or navigation grade inertial measurement units (IMU) to determine the approximated angular exterior orientation (EO) elements of images. Navigation grade IMUs, usually integrated with GNSS receivers, are also used to determine the projection center coordinates. Recent researches show that using also a low-cost attitude and heading reference system (AHRS) or a low-cost IMU, satisfies the demands of certain photogrammetric applications. Our researches aim to evaluate the accuracy of low-cost devices suitable for constructing small, low-cost photogrammetric MMS. During our research two low-cost devices, providing information about image attitude and heading, were tested. The first one is the calibrated Ricoh G700SE GPS camera with an electronic compass and a level indicator. The second device is the Xsens MTi AHRS unit, comprising 3 MEMS (micro-electro-mechanical systems) gyros, 3 MEMS accelerometers and 3 magnetometers. For the testing purposes the AHRS was combined with the calibrated Nikon D80 SLR camera. The 3D AHRS magnetometer calibration was carried out using the manufacturer's software to compensate for the soft and hard iron effects. The images of three test fields were taken. The images of the first test field with signalized control points were used to determine the boresight rotation matrix of the AHRS. The bundle adjustment was solved separately for each camera and each test field to determine the true (reference) angular exterior orientation parameters. The differences between measured and calculated angles allowed to evaluate the accuracy of the measured angles. The tests results for the GPS camera show high residuals of measured azimuths, however its level indicator allows camera levelling with sub-degree accuracy. The results obtained for the low-cost AHRS unit were significantly better, however over 2° residuals for yaw angle were also observed. The results prove the usefulness of the AHRS for constructing a small, hand-held MMS, whereas GPS camera azimuth measurements can be treated rather as a rough approximations in the photogrammetric network adjustment.

1. INTRODUCTION

1.1 Overview

The increasing number of terrestrial photogrammetric mobile mapping systems carried by vans, robots or even hand-held is being constructed. Most of them use navigation or tactical grade IMUs to measure the image EO parameters. Using such sensors makes the construction of MMSs systems expensive, therefore some alternative solutions, which allow measurements of image EO elements (especially angular ones), are met.

In this paper we would like to present our experiences with two low-cost devices able to determine the angular EO of digital images. The first one is the GPS camera with compass and tilt indicator and the second one is the MEMS AHRS unit.

First of all, we look for reasons why the measurements of the angular EO elements are useful and how such measurements were realized and utilized in the recent low-cost MMSs. Then we look closer at tested devices and the calibration procedure of the AHRS. Subsequently, the test methodology as well as results and conclusions are given.

1.2 The Role of Angular EO Measurements

The calculation of coordinates of object points from image measurements is the main task of photogrammetry. To achieve this using photogrammetric intersection, one must know the EO (and IO) elements of acquired images. The six EO elements can be determined using indirect or direct georeferencing. The indirect georeferencing often involves manual measurements of control points and is quite a time consuming process. The direct georeferencing is fast and usually takes place with a minimum additional operator work. However, the accuracies achieved using direct EO measurements (especially angular) are often insufficient for object coordinate determination. Therefore, further calculations like photogrammetric bundle adjustment are necessary to improve measured EO elements. Some of recent researches aim to work out approaches to correct measured EO elements without using control points (Bartelsen & Mayer, 2010).

In this paper, referring to angular measurements we mean always the final AHRS or IMU readouts. Nevertheless, we should keep in mind that the values of angles are determined using various devices, like magnetometers, accelerometers or gyroscopes – the individual sensors IMUs are composed of.

Below we mention few reasons the angular measurements are useful.

- a) The rotation matrix composed from measured angles is used in navigation algorithm for acceleration vector resolution.
- b) Angular (and coordinate) measurements can be used to determine object coordinates directly by means of photogrammetric intersection provided the accuracy of EO elements is sufficient for a certain application. They can also be used to project elements from the object space into the images for example to accomplish automatic texturing of 3D building models.
- c) The angular measurements can be treated as good approximations for a photogrammetric bundle adjustment. The more accurate the approximations are, the less iterations are needed. Determination of the approximated values without direct measurements is usually an awkward process. Some solutions to this problem can be found in photogrammetric handbooks (Kraus, 1997).
- d) Proving a sufficient accuracy, angular measurements can be treated as observations in a photogrammetric bundle adjustment.
- e) Measurements of the EO parameters can be used to acquire images with certain geometry (e.g. during the flight).
- f) Finally angular measurement are needed when applying the lever-arm correction. This is the case when a mobile mapping system is equipped with a GNSS antenna/receiver set. The GNSS coordinates should be corrected for the antenna – projection centre offset.

In this paper we try to analyse which of above given tasks can be realized using the tested low-cost AHRS devices.

1.3 Related work

In the last decade some tests of mobile mapping systems comprising cameras, GNSS sets and low-cost AHRSs, were conducted. Ellum & El-Sheimy (2001) and Coppa et al. (2007) present a backpack mobile mapping system. They used a Leica DMC-SX digital compass with an inclinometer to sense all three angles. The reported RMSE of measured angles were about 0.7° , 0.4° , 0.7° , respectively for *roll*, *pitch* and *yaw*. However, about 10° residuals for *yaw* angle were also reported. This was caused most likely by some magnetic disturbances. The measured angles were used to determine the object point coordinates by means of a combined bundle adjustment (application d.). It was not mentioned if the lever-arm correction (application f.) was carried out.

Haala & Boehm (2003) present a telephoning device used for navigation in cities. The main task was to match the building contours observed in the images with building models kept in a database. The attitude and heading information was provided by an inclinometer ($1\div 2^\circ$ error) and a digital compass ($0.6\div 1.5^\circ$ error). The coordinates were determined by GPS. Measured EO elements were used to project approximately the building contours into the images (application b.). The line matching was performed for further vector-to-image alignment.

Besides digital compasses, a mid-cost tactical grade IMUs/AHRSs using mainly fiber optic gyros (FOG) are used for attitude and heading determination. Costs of such devices are approximately 2 to 8 times higher than costs of magnetometers-based low-cost AHRS, but are still below costs of a navigation-grade IMUs. Piras et al. (2008) describe a van MMS comprising a cheap webcam, 2 GNSS dual-frequency receivers and a fiber optic tactical grade IMU with $20^\circ/\text{h}$ bias. The systematic *yaw* gyro drift is compensated using the azimuth of the segment between two GPS antennas. Similar idea, but without using IMU, is realized by Da Silva et al. (2003). In both systems the measured EO elements are used directly for intersection (application b.). The lever-arm correction had to be applied as well. Mentioned works proved the usefulness of low- and mid-cost AHRSs for certain photogrammetric applications but also showed their weak sides. The sensors based on magnetometers can perform well for a long time, but can suddenly give wrong *yaw* readout when a magnetic disturbance of any kind occurs. The *roll* and *pitch* measurements tend to be much more stable as their values are calculated not only from gyro but also from local gravity vector components. On the other hand, mid-cost IMUs have significant gyro drift which must be compensated in some other way. In the near future the low-cost AHRSs will take advantage of the further development of the MEMS technology (El-Sheimy, 2009), so better performance of low-cost IMUs is expected.

2. TESTED DEVICES

2.1 GPS Camera

The tested GPS camera is Ricoh G700SE. Besides GP-1 mode, the camera is equipped with digital compass and inclinometer. The geometric resolution is 3000×4000 pixels. The

CCD sensor has a 1/2.3" format. Images have visible noise even if low sensitivity (ISO 100) is set. The camera was calibrated.

Using Ricoh GPS camera we cannot measure all three orientation angles. We have only the readouts of camera axis azimuth and we can judge if the camera is tilted or not. Our tests aim to evaluate the accuracy of measured azimuth and check how accurate is the digital level indicator.

2.2 AHRS

The second tested device is Xsens MTi AHRS unit. The unit can be regarded as a full 3D IMU because it consists of 3 accelerometers, 3 gyros and, additionally, 3 magnetometers. We used this IMU to sense three rotation angles only. According to the product specification we should expect the accuracy of about $1.0/0.5/0.5^\circ$ for *yaw*, *pitch* and *roll* respectively in the static mode (no accelerations). The *yaw* accuracy is worse as its value is calculated from magnetometers indications. *Roll* and *pitch* are determined from the local vertical vector components sensed by accelerometers. When the AHRS is subjected to accelerations, the *roll* and *pitch* are still tracked using gyros. Gyros prevent also from errors caused by sudden magnetic disturbances which is important especially in the cities where many ferromagnetic materials (cars, building constructions) can be met. The sensor is able to track the orientation in a reference frame defined by a local vertical and magnetic north direction. All measurements are integrated using Kalman filter.

The AHRS unit was mounted on a small platform together with the Nikon D80 SLR camera (Fig. 1). The coordinate frames of the camera and the AHRS unit were aligned approximately mechanically. The camera reference frame is rotated with respect to the AHRS frame by 90° about the X axis. The boresight rotation matrix was calculated for the camera to take account on the remaining small misalignment.

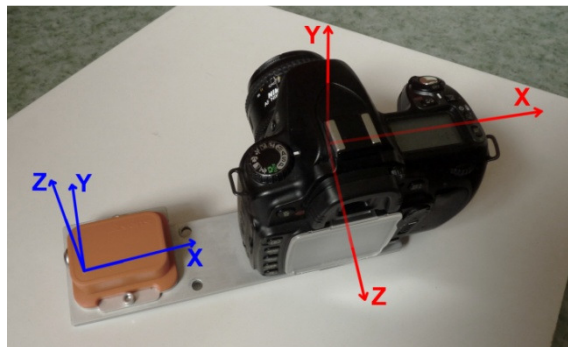


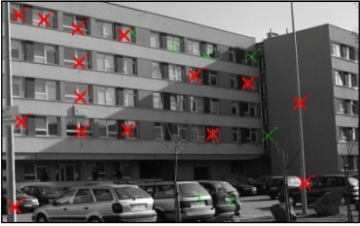
Fig. 1. The configuration of the AHRS unit and SLR camera.

3. CALIBRATION AND TEST FIELDS

For our tests and calibration we used altogether three test fields. Exemplary images and control point quantity are given in the Table 1. Test field image screenshots contain measured control and tie points. Test field #1 was used for a boresight calibrations of the AHRS unit. Images for the AHRS tests were taken in the second and third test field. Test

images for GPS camera were taken only in the first test field. The control point coordinates were determined in the Polish Coordinate System ‘2000’ (EPSG:2178). We used the ellipsoid elevation system.

Tab. 1. Test fields used during researches. Red marks – control points, green marks – tie points.

	Image	GCPs & purpose
Test field #1		36 signalized control points. Test field used for AHRs boresight calibration and GPS camera test.
Test field #2		12 natural ground control points. Test field used for AHRs test.
Test field #3		30 natural ground control points. Test field used for AHRs test.

4. SENSOR CALIBRATION

4.1 Notes on camera calibration

When the measured EO elements are going to be incorporated in the bundle adjustment as observed values, it is very important to apply the adequate lens distortion model. In the over-parameterized model a large correlations between EO and IO parameters can be observed, so that calculated EO parameters are not consistent with physical values. If insufficient number of camera parameters (distortion coefficients) is used, similar effect can be observed. Therefore for the test purposes it was important to use optimal distortion

model. The Brown's k_1, k_2, p_1, p_2 coefficients were estimated for the GPS camera and only k_1 and k_2 coefficients for the Nikon D80 SLR camera with the 20 mm lens.

4.2 Calibration of Magnetometers

As the SLR camera mounted on the platform consists of ferrous materials, the magnetic calibration according to principle given by Caruso (1997) was performed. The results show that the soft iron effect is present and the magnetometer corrections should be taken into account to compensate for it. The calibration of the GPS camera digital compass was also performed according to the user manual.

4.3 Boresight Calibration

Even though the mechanical alignment was made carefully, coordinate systems of camera and unit are not aligned precisely. In order to treat the angles measured by the AHRS as the image angular EO elements, we should correct them (1). In practice we calculate a rotation matrix R_{IMU} from the AHRS measurements. Then we multiply it by the object alignment matrix (R_{ALN} -90° rotation about the camera X axis). Finally we use the boresight rotation matrix (B), which is usually close to the identity matrix. As a result we obtain a camera rotation matrix (R_{PHOTO}). We can now calculate the corrected camera Euler angles directly from R_{PHOTO} .

$$R_{PHOTO} = R_{IMU} R_{ALN} B \quad (1)$$

The IMU *yaw* readouts are corrected for magnetic declination (NOAA, 2010) and convergence. These corrections are assumed to be constant for small areas. The local vertical deflections were not taken into account as their components are much smaller than AHRS accuracies.

Tab. 2. Differences between reference and measured angles after applying estimated AHRS boresight correction.

Image	v_a [°]	v_v [°]	v_k [°]
1	0.192	0.085	0.111
2	0.503	-0.101	0.347
3	-0.068	-0.002	0.227
4	-0.475	-0.120	0.081
5	0.211	-0.070	0.157
6	-0.796	0.082	0.084
7	-0.881	-0.021	-0.159
8	-0.491	-0.050	-0.287
9	0.040	0.014	-0.045
10	0.379	0.041	-0.124
11	0.403	-0.093	-0.256
12	0.165	0.019	-0.075
13	0.328	0.096	-0.168
14	0.527	0.133	0.055
RMSE	0.458	0.078	0.179

The functional model we used for boresight calibration is nearly the same as model described by Bayoud (2006). We took 14 images of our test field. One of them is shown in the Table 1. To obtain the reference rotation matrix entries the photogrammetric network with control and tie points was adjusted. The boresight rotation matrix was estimated. The differences between reference and measured values after applying estimated boresight correction are given in the Table 2. The image angles are recalculated to the *alpha-nu-kappa* Euler rotation system (Kraus, 1997). The highest differences are observed for the α angle because it depends on the *yaw* angle mostly.

5. TESTING

5.1 GPS Camera

We took 9 pictures of the test field #1 using the GPS camera. During the image acquisition the *kappa* angle was kept close to zero according to the level indicator. Using level indicator we were not able to judge if the camera *nu* angle is close to 90°. 26 GCPs were measured. Afterwards we performed the bundle of the image network. The calculated angular EO parameters were treated as reference values for the comparison. As earlier, the *alfa-nu-kappa* rotation system was applied. The differences between measured and calculated *alpha* angles as well as the *kappa* values are given in the Table 3.

Tab. 3. Differences between reference and measured angles for the GPS camera. Test field #1.

Image ID	ν_α [°]	κ [°]
1	≈ -25	-0.37
2		-0.86
3		-0.75
4		-0.52
5		-0.50
6		-0.08
7		-0.04
8		-0.85
9		-0.93
Mean value	-	-0.54
σ_m	-	0.11

5.2 AHRS

The location of 10 image stations at test field #2 is shown in the Figure 2. For images 16-20, the camera to façade distance was about 12 m. For the images 21-25 the distance from a façade was 25 m. Besides 12 control points we measured 32 tie points. We corrected the measured angles using estimated boresight rotation matrix. Then we calculated the bundle adjustment. Estimated *alpha*, *nu* and *kappa* angles were compared with measured values. The differences are shown in the Table 4.

We took 24 images of test field #3 (Fig. 3). The camera to object distance was about 3÷4 metres. 26 ground control and 69 tie points were measured in the images. The bundle

adjustment was calculated to compare true and measured values of the angular EO elements. The results of the comparison are given in the Table 5.

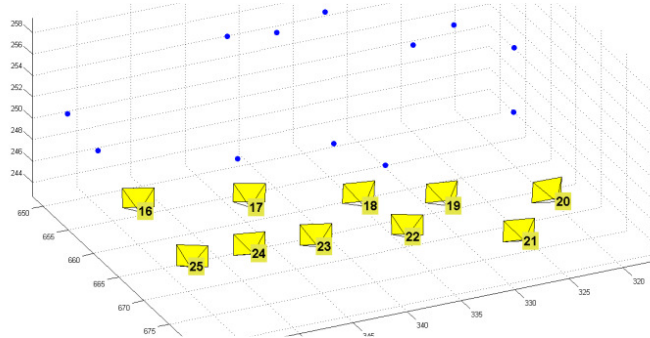


Fig. 2. Camera stations and GCPs in the test field #2.

Tab. 4. Differences between reference and measured angles for the AHRS. Test field #2.

Image ID	v_α [°]	v_γ [°]	v_κ [°]
16	0.554	0.008	0.167
17	0.382	-0.040	0.348
18	0.890	0.016	0.220
19	0.953	0.085	0.209
20	1.704	0.070	0.099
21	2.444	0.035	0.126
22	2.291	0.078	0.163
23	4.529	0.010	0.177
24	5.327	0.039	-0.047
25	3.542	0.107	-0.099
Mean value (m)	2.262	0.041	0.136
σ_m	0.543	0.014	0.041

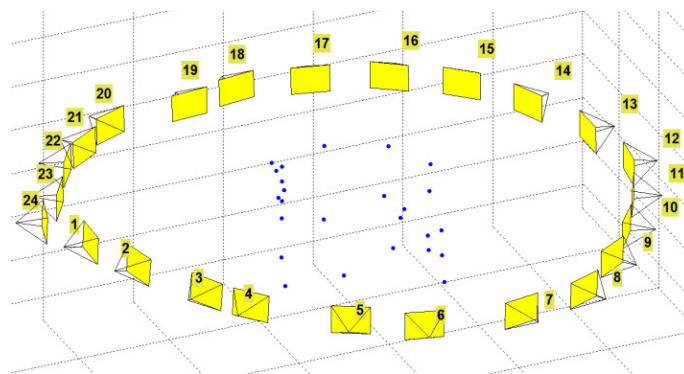


Fig. 3. Camera stations and GCPs in the test field #3.

Tab. 5. Differences between reference and measured angles for the AHRS. Test field #3.

Image ID	v_α [°]	v_γ [°]	v_κ [°]
1	-0.069	-0.064	0.129
2	1.797	-0.016	-0.087
3	-1.468	0.017	-0.308
4	-2.074	-0.019	-0.240
5	-1.789	-0.113	-0.352
6	-1.425	-0.009	-0.121
7	-7.421	-0.128	-0.235
8	-2.935	0.025	-0.138
9	3.287	-0.037	-0.037
10	2.146	-0.013	-0.156
11	1.620	-0.039	-0.011
12	1.159	-0.136	0.096
13	0.098	-0.138	-0.084
14	0.466	-0.056	-0.074
15	1.142	-0.088	0.040
16	2.173	-0.041	-0.494
17	2.413	0.116	-0.195
18	0.971	-0.058	-0.073
19	0.622	-0.017	-0.042
20	0.947	-0.022	-0.091
21	0.536	-0.026	-0.143
22	0.124	0.001	-0.105
23	-1.235	-0.067	-0.054
24	-1.124	-0.080	-0.031
Mean value (m)	0.321	-0.038	-0.112
σ_m	0.338	0.012	0.029

6. DISCUSSION

We observed very high differences (about -25°) of the *alpha* angles for the GPS camera. Such high values were unexpected and we cannot find any reasonable explanation of this phenomenon. One of possible explanation is a misalignment of compass and lens optical axis. The second is a strong ferromagnetic effect, however it should not be present because of the compass calibration performed according to the user guide. We repeated the compass calibration and measurement and obtained even worse results. In contrary to *alpha* differences, *kappa* differences are small. We expected over 1° *kappa* values whereas all of them are smaller and all of them are negative. About -0.5° misalignment of level indicator and camera XZ axes plane is observed (Table 3, mean values). In further researches it should be checked if this systematic error is repeatable from camera turn on to turn on.

The results obtained for the Ricoh GPS camera show that measured *alpha* angles can be treated only as rather rough approximations (application c.), whereas the level indicator allows us to make images with *kappa* angle close to zero. This can be used e.g. for stereo

image acquisition (application e). The second *nu* level indicator (the camera is unfortunately not equipped with) would be useful to acquire nearly normal images. The differences obtained for the AHRS *yaw/alpha* angle are much smaller than for GPS camera. According to the manufacturer's specification we should expect *yaw/alpha* error not higher than 2° in dynamic and 1° in static mode. The differences smaller than this values were observed only during the boresight calibration (Table 2). The value of 2° was exceeded during both tests for many images. On the other hand, much higher residual values were observed in similar test with digital compass (Ellum & El-Sheimy, 2001). In Table 4 we see that all differences for the *alpha* angles are positive, however in Table 5 and Figure 4 we see that the differences change non-randomly from image to image. There is no systematic error of *yaw* angle (see σ value of the mean difference in Table 5). Negative values are observed for images 3 to 8, whereas positive values are observed on the opposite side of the test field object (15-18) and also for images 9 to 12. One of the possible reasons of this phenomenon is the presence of ferrous materials in the construction of the building the images were taken around. The magnetic calibration of the AHRS should also be repeated with a higher number of samples, because such errors can come from the uncompensated iron effect caused by the SLR camera.

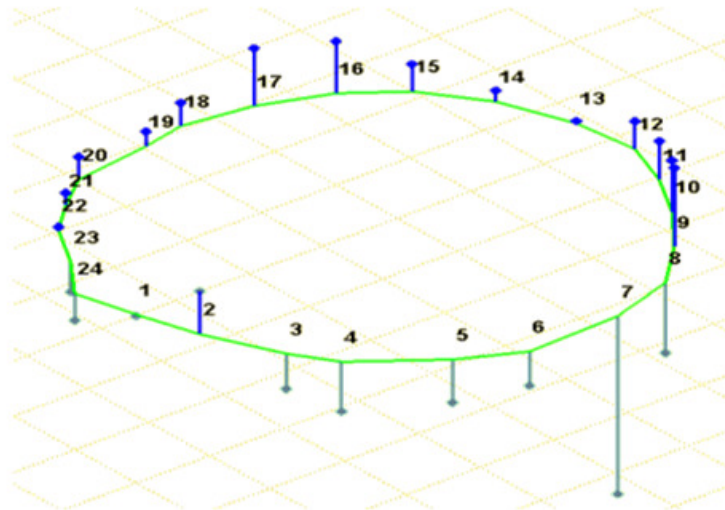


Fig. 4. Differences of the *alpha* angles in test field #3. Blue lines are proportional to values in the Table 4.

The residuals of *nu* and *kappa* angles are much below the limit given in the product specification. For each test measurement we observe systematic biases. However, it should be noted that these biases are not stable and change from turn on to turn on of the device. The negative systematic errors of *nu* and *kappa* are observed for the test field #2. Positive systematic errors are observed for the test field #3.

The results of researches show that after applying the boresight correction the accuracy of image angles seems to be sufficient to treat them as observations in photogrammetric

network adjustment (application d). Weights assigned to *yaw* angles must be smaller than *nu* and *kappa* weights. The Xsens MTi unit is also an appropriate device for constructing the low-cost MMS with a GNSS antenna. The observed angles are accurate enough to apply the lever arm correction i.e. shifting of the GNSS antenna phase centre coordinates to the image projection centre (application f.). In such a system the camera should be placed directly below the antenna. In this case the influence of the *yaw* error on the error of the lever arm vector would be minimized.

The results of these researches show the usefulness of a low cost AHRS for constructing a small MMS for terrestrial photogrammetry. Using a dual frequency RTK GPS set, favourable image configuration and sufficient number of tie points is expected to compensate for lower accuracy of angular measurements.

ACKNOWLEDGEMENTS

The study has been carried out with financial support from the statutory research AGH no. 11.11.150.949 and 11.11.150.005.

Both authors are scholarship holders of the project “Doctus – Małopolski fundusz stypendialny dla doktorantów”.

REFERENCES

- Bartelsen, J., Mayer M., 2010. Orientation of Image Sequences Acquired from UAVs and with GPS Cameras, International Calibration and Orientation Workshop EuroCOW 2010, Castelldefels, Spain.
- Bayoud, F.A., 2006. Development of a Robotic Mobile Mapping System by Vision-Aided Inertial Navigation: A Geomatics Approach, Geodaetisch-geophysikalische Arbeiten in der Schweiz, Schweizerischen Geodaetischen Kommission.
- Caruso, M.J., 1997. Application of Magnetoresistive Sensors in Navigation Systems. *Sensors and Actuators*, SAE SP-1220, pp. 15-21.
- Coppa, U., Guarnieri, A., Pirotti, F., Vettore, A., 2007. A Backpack MMS Application, The 5th International Symposium on Mobile Mapping Technology, Padua, Italy.
- Da Silva, J.F.C., de Oliveira Camargo, P., Gallis, R.B.A., 2003. Development of a Low-Cost Mobile Mapping System: a South American Experience, *The Photogrammetric Record*, 18(101), pp. 5-26.
- Ellum, C.M., El-Sheimy, N., 2001. A Mobile Mapping System for the Survey Community, Proceedings of the 3rd International Symposium on Mobile Mapping Technology, Cairo, Egypt.
- El-Sheimy, N., 2009. Emerging MEMS IMU and Its Impact on Mapping Applications, Photogrammetric Week '09, Dieter Fritsch (Ed.), Wichmann.
- Haala, N., Boehm, J., 2003. A multi-sensor system for positioning in urban environments, *ISPRS Journal of Photogrammetry & Remote Sensing*, 58(1-2), pp. 31-42.

Kraus, K., 1997. *Photogrammetry. Vol. 2, Advanced Methods and Applications*. Ferd. Duemmlers Verlag, Bonn, pp. 15-17, 43-59.

NOAA, 2010. Magnetic Field Research Model.
<http://www.ngdc.noaa.gov/geomag/EMM/index.html> (accessed 15 Apr. 2011).

Piras, M., Cina, A., Lingua, A., 2008. Low cost mobile mapping system: an Italian experience, ION/IEEE Position, Location, and Navigation Symposium, ION/IEEE PLANS 2008, Monterey, USA.